

Magnetic properties of UPt_3 in the superconducting state

Andreas Amann* and Ana Celia Mota

Laboratorium für Festkörperphysik, ETH-Hönggerberg, CH – 8093 Zürich, Switzerland

M. Brian Maple

UCSD, IPAPS-0360, 9500 Gilman Drive, La Jolla, California 92093-0360

Hilbert v. Löhneysen

Physikalisches Institut, Universität Karlsruhe, D – 76128 Karlsruhe, Germany

(Received 19 September 1997)

The unconventional phase diagram of superconducting UPt_3 has been explored using measurements of magnetic properties at low external fields. We investigated the relaxation of vortices from metastable configurations as well as the low-field ac magnetic susceptibility χ . The data yield a clear distinction between the behavior of vortices in the two low-field phases A and B. In the high-temperature A phase, vortices trapped in the bulk of the specimen after cycling it in a magnetic field creep out as expected with a rate which increases with increasing temperature. Bulk vortices in the B phase, on the other hand, remain so strongly pinned that no creep could be detected for those vortices. This behavior indicates that an intrinsic and very effective pinning mechanism exists in the low-temperature superconducting phase of UPt_3 . Furthermore, a rather small dissipation peak at the lower transition temperature T_c^- could be detected in the out-of phase component of the magnetic ac susceptibility. Both these effects can be well explained with the notion that the low-temperature, low-field B phase of UPt_3 is characterized by a superconducting order parameter which breaks time-reversal symmetry. [S0163-1829(98)04306-9]

I. INTRODUCTION

Ever since the discovery of superconductivity in the heavy-fermion compounds, the question of its exact nature and origin has attracted great interest. As of today, six superconducting heavy-fermion compounds are known, all of them having transition temperatures T_c between 0.5 and 2 K. Early data showing unusual temperature dependences of the heat capacity, penetration depth, and sound absorption led to the postulate that the superconductivity in some of these compounds is of an unconventional nature, i.e., characterized by a reduced symmetry of the order parameter. Among all of these superconductors, UPt_3 holds a special place due to the well established presence of more than one superconducting phase — in analogy to the phase diagram observed for superfluid ^3He . The phase diagram of UPt_3 is nowadays known in great detail after careful experimental investigations.¹ Three different superconducting phases, labeled A, B, and C, are observed in the H - T plane. However, none of the existing phenomenological models describing the order parameter of UPt_3 and its symmetry can completely explain all available experimental data. It is therefore necessary to look into new phenomena and carry out different types of experiments in order to reach an unambiguous identification of the observed superconducting phases.

Some efforts toward such an identification have concentrated on effects due to the breakdown of additional symmetries besides the gauge symmetry-breaking characteristic of a BCS superconductor.² As discussed extensively by Sigrist and Ueda,³ time-reversal symmetry-breaking superconducting phases should exhibit various magnetic effects which are not found in conventional superconductors. In particular, the

mixed phases of a superconductor with a multicomponent order parameter should exhibit nontrivial structures with fractionally quantized vortices in domain walls between domains of degenerate superconducting phases and nonaxial vortices in the bulk of these domains.

The present work focuses on the investigation of relaxation of vortices from metastable configurations, i.e., the decay of the remanent magnetization trapped in a sample after cycling it in a magnetic field. Previous investigations of flux dynamics at low fields yielded that the relaxation of the magnetization towards equilibrium in UPt_3 is clearly distinct from the one observed in classical or high-temperature superconductors.⁵ In the present work we have extended the magnetic measurements in order to explore in detail the two low-field phases of UPt_3 .

The study of flux dynamics has been performed in two different samples of UPt_3 , namely, a single crystal and a sintered granular sample. In order to check whether the effects observed are really signatures of the unconventional phase diagram of UPt_3 , the same type of measurements has also been performed in a crystal of UPe_{13} , another heavy-fermion superconductor which — in its pure chemical form — does not show multiple superconducting transitions.

Furthermore, a detailed investigation of the low-field ac magnetic susceptibility has been performed on the UPt_3 single crystal taking advantage of the high sensitivity of our measuring system based on a superconducting quantum interference device (SQUID) magnetometer. Apart from measurements of the superconducting transition at T_c^+ , the investigation was focused on the lower superconducting transition at T_c^- . To our knowledge, this transition has, up to now, never been detected in magnetic susceptibility measurements.⁴

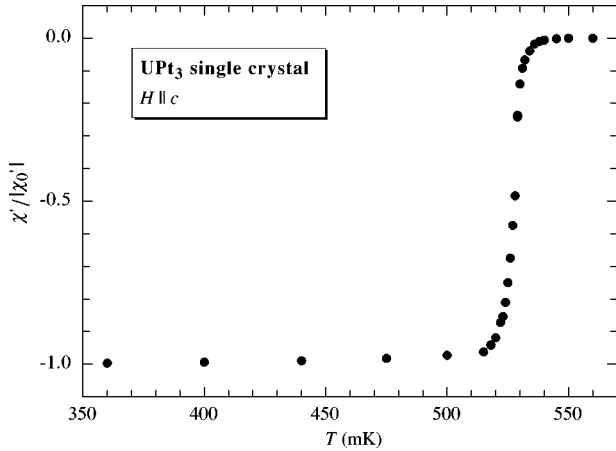


FIG. 1. In-phase component of the ac magnetic susceptibility of the UPt_3 single crystal. The data have been taken with an ac amplitude $H_{\text{ac}}=6.6$ mOe in the residual field of the cryostat $H_{\text{dc}}^{\text{res}} < 2$ mOe; the susceptibility has been renormalized using the minimal value of the susceptibility χ' at the lowest temperature $\chi'_0 = \chi'(T \rightarrow 0)$.

II. EXPERIMENTAL DETAILS

A. Measuring setup

All measurements reported here were performed using a ^3He - ^4He dilution refrigerator where the sample is in direct contact with the ^3He - ^4He mixture inside the mixing chamber of the refrigerator. Ultrasensitive measurements of magnetic properties were performed using rf-SQUID magnetometers. In our system, the samples stay stationary inside the detection coils during all measurements. Thus, inhomogeneities in either the applied or the residual field in the cryostat have no influence on the measurements.

The residual field at the sample space has been measured to be less than 2 mOe. The dc field can be varied up to about 2500 Oe. For the ac susceptibility measurements, an ac impedance bridge with a SQUID as a null detector is used. The amplitude of the ac field can be varied in nine fixed steps from 0.07 up to 33 mOe, and its frequency can be chosen from four different values between 16 and 160 Hz.

B. Samples

For the work presented herein, two different UPt_3 samples have been investigated, namely a single crystal and a sintered granular sample. The single crystal was prepared from arc-cast polycrystalline rods by zone melting in high vacuum. Laue x-ray-diffraction analysis was used to orient the single crystal which was then cut into smaller pieces with a diamond wheel saw. Thereafter, it was annealed in vacuum at 800°C for six days. The sample has a mass of 68.2 mg and is $1.5 \times 2.9 \times 0.9$ mm³ in size, with the c axis pointing along the shortest dimension of the crystal.

The transition temperature of the single crystal has been obtained from ac magnetic susceptibility measurements (Fig. 1) as well as from specific-heat measurements (Fig. 2). From the susceptibility data, the superconducting transition takes place at $T_c^+ = 528$ mK with a width ΔT_c^+ of about 11 mK. Here T_c^+ has been taken as the midpoint of the tran-

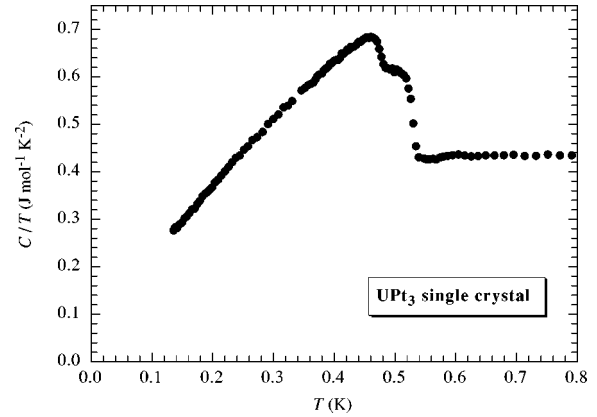


FIG. 2. Ratio $\gamma(T) \equiv C/T$ of the specific heat (measured in zero external field) over temperature as a function of temperature showing two clearly separated jumps in the specific heat at the two transition temperatures $T_c^+ = 529$ mK and $T_c^- = 476$ mK. From the data above the upper transition temperature T_c^+ , the coefficient in the normal state $\gamma(0) = 433$ mJ mol⁻¹ K⁻² can be extracted. The quality of the single crystal is reflected in the value of the linear extrapolation of C/T in the superconducting state yielding $\gamma^*(0) \approx 75$ mJ mol⁻¹ K⁻².

sition and the value for ΔT_c^+ results from using the 10–90 % criterion. The two specific-heat jumps give $T_c^+ = 529$ mK and $T_c^- = 476$ mK.

In order to study surface effects on superconducting UPt_3 , a sintered granular sample has been investigated. The grains have an average diameter of about $7 \mu\text{m}$ and have been annealed and sintered into a cylindrical shape at 1000°C for two days. This sample has a mass of 133 mg, a diameter of 3.3 mm, and a height of 1.3 mm.

The ac susceptibility transition into the superconducting state of the granular sample is significantly wider than the one of the single crystal and it starts at a considerably lower temperature as shown in Fig. 3.

III. RESULTS

A. Magnetic susceptibility at $T \approx T_c^-$

Careful measurements of the ac susceptibility were performed in the vicinity of T_c^- , the lower superconducting

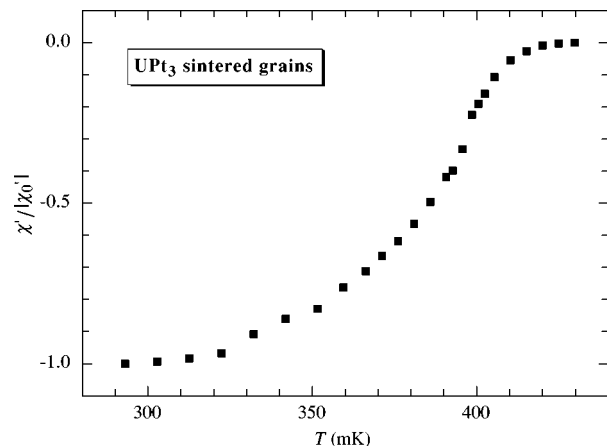


FIG. 3. ac magnetic susceptibility of the sintered granular UPt_3 sample. The measuring parameters are the same as the ones used for the single crystal (see Fig. 1).

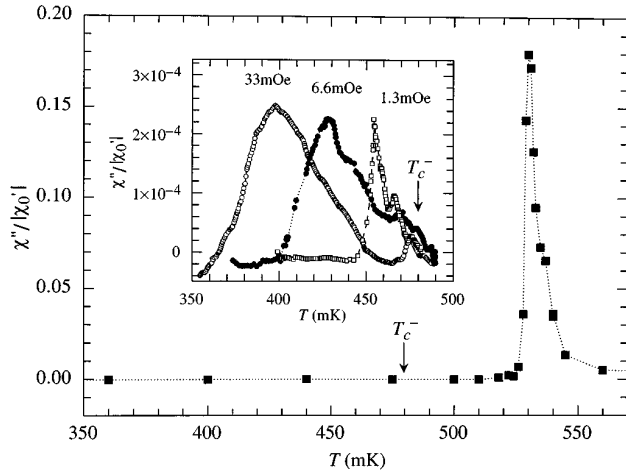


FIG. 4. Out-of-phase component χ'' of the ac susceptibility of the UPt₃ single crystal measured with an amplitude $H_{ac}=6.6$ mOe in a residual dc field $H_{dc}^{res}<2$ mOe. In the inset, an enlargement of the region around $T=450$ mK for different amplitudes H_{ac} of the measuring field is shown. The arrows in both graphs indicate the upper onset of the lower transition temperature T_c^- at a temperature $T\approx 480$ mK as determined from specific-heat measurements on the sample (see Fig. 2).

transition temperature. In Fig. 4, we show the out-of-phase component χ'' of the ac susceptibility of the UPt₃ single crystal in the orientation $H_{ac}\parallel c$. The peak at the superconducting transition T_c^+ shows a shoulder at high temperatures and falls sharply as the temperature is reduced below T_c^+ . Well separated from the transition at T_c^+ , an unexpected second peak appears as shown in the inset of the Fig. 4. The size of this second peak is about 1/300 of the size of the peak in χ'' at T_c^+ which probably explains why it has not been reported up to now in less sensitive measurements.

Between 16 and 160 Hz, the extremely small peak in χ'' does not depend on the frequency of the measuring field. On the other hand, while the position and width of the peak in χ'' at T_c^+ are practically independent of the amplitude H_{ac} of the measuring field (at least for the amplitudes used in our measuring system), the maximum of the second peak moves rapidly towards lower temperatures and the peak widens with increasing amplitude H_{ac} as shown in the inset of Fig. 4 and in Fig. 5. It is clear that the strong reduction in temperature of the peak's maximum with ac field ($dH_{ac}/dT\approx 0.6$ Oe/K) cannot be compared with the field dependence of the boundary between the A and B phases having a slope $dH_c/dT\approx 1.4\times 10^6$ Oe/K for $H\parallel c$. Likewise it cannot be attributed to a phase of slightly different stoichiometry considering the difference of more than five orders of magnitude in the dH/dT slopes.⁴ The onset of the small peak in χ'' is independent of H_{ac} , and it occurs at $T\approx 480$ mK. Based on the established phase diagram of UPt₃ and considering the good agreement of this temperature with the value of T_c^- obtained from our specific-heat measurements on the same single crystal, we identify the *onset* of the second dissipation peak with the lower transition temperature T_c^- .

A second weak peak developing at $T\leq T_c^-$, temperatures at which the specimen is *fully* superconducting, has no trivial interpretation. Most likely it is related to hysteresis losses

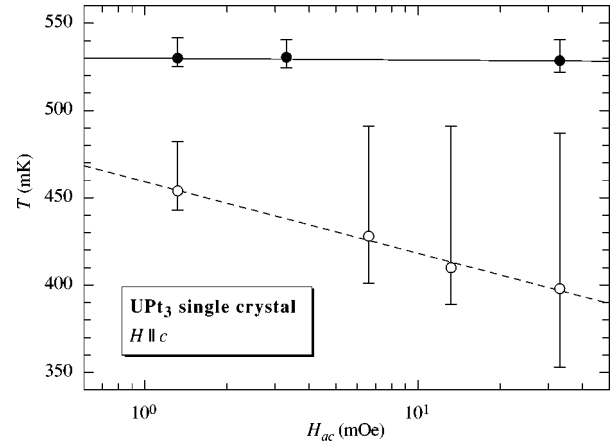


FIG. 5. Widths and positions of the maxima of the peaks in the out-of-phase component χ'' of the ac susceptibility of the UPt₃ single crystal at T_c^+ (●) and at T_c^- (○). The circles denote the positions of the maxima, the vertical lines indicate the widths of the peaks. The dashed and solid lines serve only as guides to the eye.

which are not present at temperatures above T_c^- . In several studies of the complex ac susceptibility in sintered high- T_c superconductors it has been shown that the imaginary part χ'' of the susceptibility exhibits two peaks below T_c , one corresponding to bulk pinning hysteresis losses and a second peak resulting from losses due to the motion of intergranular Josephson vortices. The second peak is independent of frequency in the range .01–10 kHz, and its maximum shifts rapidly to lower temperature with increasing ac field amplitude. For example, for a sintered sample of Y-Ba-Cu-O, Goldfarb *et al.*⁶ measured $dH_{ac}/dT=0.6$ Oe/K. Both dissipation peaks extrapolate to $T=T_c$ for $H_{ac}\rightarrow 0$. This behavior at weak magnetic fields ($H\ll H_{c1}$) has been well described in terms of a critical state model for granular superconductors by Müller.⁷

In the inset of Fig. 4, we observe rather similar dissipation peaks. However, contrary to the case of granular Y-Ba-Cu-O, the weak peak in χ'' starts to develop *only below* T_c^- , the temperature corresponding to the boundary between the A and B phases. Based on this, we interpret the origin of dissipation below T_c^- in the bulk material as due to the formation of superconducting domains in the low-temperature phase. Such domains are expected to occur in the B phase if that phase breaks time-reversal symmetry.^{3,8} Dissipative processes can arise in domains separated by domain walls from spontaneous currents and motion of weakly pinned vortices as well as domain walls. On further reducing the temperature, the domain walls and vortices are more strongly pinned, so that the maximum in χ'' is pushed towards lower temperatures for higher H_{ac} amplitudes.

B. Magnetization measurements

UPt₃ single crystal

Bulk isothermal dc magnetization curves were measured using the SQUID magnetometer for all samples. A magnetization cycle of the UPt₃ single crystal recorded with $H\parallel c$ is shown in Fig. 6. From the shape of the magnetization curve one can infer the presence of strong flux pinning. As a con-

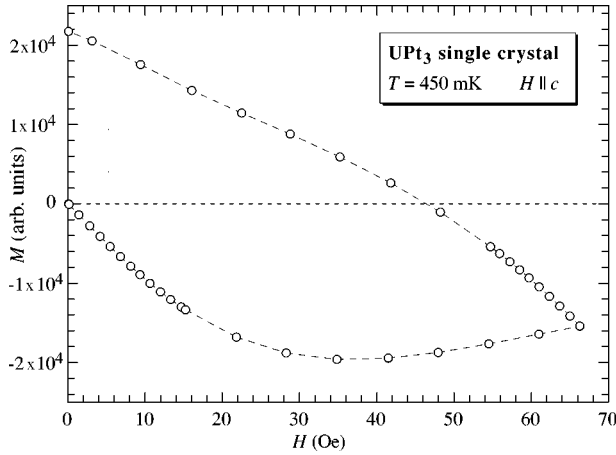


FIG. 6. dc magnetization curve of the UPt₃ single crystal at a temperature $T = 450$ mK.

sequence of pinning, the magnetization for increasing fields shows a rather wide cusp instead of a sharp minimum at the lower critical field H_{c1} .

From a quantitative analysis of the magnetization curves, values for the remanent magnetization M_{rem} trapped inside the sample at the end of a magnetization cycle can be obtained. In Fig. 7, values of M_{rem} of the single crystal for two field directions ($H \parallel c$ and $H \perp c$) are shown as functions of temperature; all the points in this figure have been taken with the specimen cycled to sufficiently high fields, so that the remanent magnetization was independent of the cycling field H^{max} , i.e., with the sample being in the fully critical state. Thus, the remanent magnetization M_{rem} of the sample is directly proportional to its critical current j_c , with a proportionality factor which depends only on the geometry of the sample. For instance, for the simplest case of an infinite superconducting slab of thickness d one obtains⁹

$$M_{\text{rem}} = \frac{d}{4} j_c. \quad (1)$$

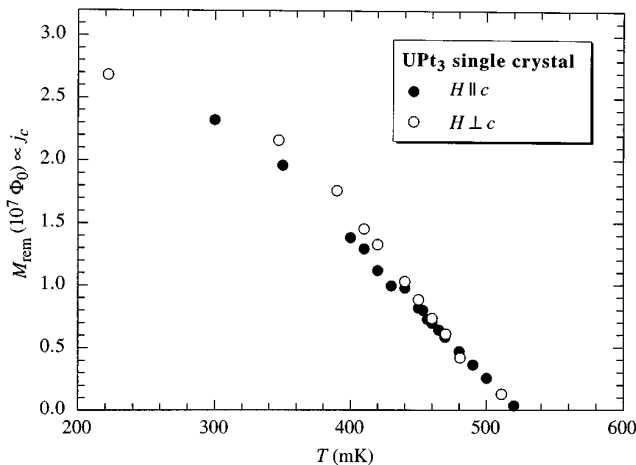


FIG. 7. Remanent magnetization of the UPt₃ single crystal in the fully critical state for the two field directions $H \parallel c$ (●) and $H \perp c$ (○). The remanent magnetization M_{rem} is given in number of flux quanta Φ_0 at the sample.

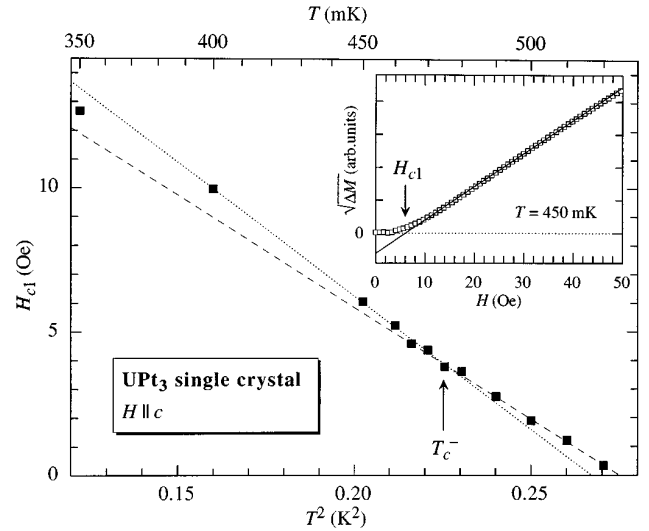


FIG. 8. Values of the lower critical field H_{c1} as obtained from magnetization curves of the UPt₃ single crystal with $H \parallel c$ as function of the square of the temperature. The two lines represent linear fits [corresponding to a temperature dependence as in Eq. (2) for H_{c1}] using only the points at high (low) temperature. The two lines cross each other at a temperature $T = 475 \pm 10$ mK (note that the values for H_{c1} are *not* corrected to account for demagnetization effects). In the inset, the method used to obtain H_{c1} is illustrated using the data of a magnetization curve taken at $T = 450$ mK (see text for details).

Due to the large pinning, the determination of the lower critical field H_{c1} is not straightforward since the minimum of the increasing branch of the magnetization curve lies at a value considerably higher than H_{c1} . Moreover, the initial slope of the magnetization cycle always shows some curvature. This results from the fact that, due to demagnetization effects, the field is greatly enhanced at the corners of the sample, so that flux can penetrate into the sample through corners already for very small applied fields. Thus, no field of first flux penetration H_p could be extracted from the data by simply defining the point where the deviation ΔM from the initial slope of M versus H takes place. However, using the simple model of Bean⁹ for the magnetization of a type-II superconductor, which predicts that the magnetic induction of the sample increases quadratically for fields $H > H_{c1}$, a quantitative analysis of H_{c1} is possible: plotting the square root of the deviation ΔM versus the applied field H yields a line intersecting the H axis at $H = H_{c1}$. In Fig. 8, the results obtained for the lower critical field are plotted against the square of the temperature. In the inset of the figure, the method of analysis explained above is illustrated for one magnetization cycle.

The H_{c1} data in Fig. 8 cannot satisfactorily be fitted with a single temperature dependence of the form

$$H_{c1}(T) = H_{c1}(0) \left[1 - \left(\frac{T}{T_c} \right)^2 \right] \quad (2)$$

over the whole temperature range but only using two slightly different values of $H_{c1}(0)$ and T_c for the high- and low-temperature regimes. The two fits to the lowest and highest points respectively, cross each other at a temperature $T = 475 \pm 10$ mK which coincides well with the lower transi-

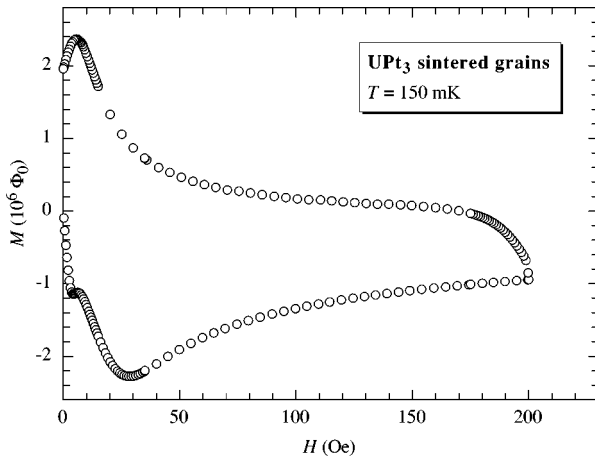


FIG. 9. Magnetization cycle of granular UPt_3 at a temperature $T=150$ mK. The magnetization M is given in number of flux quanta Φ_0 at the sample.

tion temperature $T_c^- = 476$ mK as obtained from the specific-heat measurements of this sample. A kink in the temperature dependence of the lower critical field of UPt_3 has already been reported by other groups.^{10,11} In those works, however, the temperature where the kink was observed does not agree with the measured lower transition temperature T_c^- for those samples but occurs at a significantly lower temperature.

Sintered granular UPt_3 sample

In Fig. 9, a magnetization curve of the sintered granular sample of UPt_3 is shown. For low fields, an anomalous behavior can be seen for increasing as well as for decreasing fields. For increasing fields, the initial slope changes rather abruptly to less than half its initial value at $H \approx 5$ Oe. For decreasing fields a change of sign of the slope takes place at about the same field. Both features can easily be explained to result from the so-called intergrain Josephson currents: when a magnetic field is applied, it induces shielding currents, which can run not only within single grains but also between them. Thus, at low fields shielding currents can run all around the sample. On increasing the external field, the shielding currents grow until the Josephson contacts between the individual grains can no longer sustain them. The field H_J at which the induced intergranular currents break down (i.e., roughly speaking, the field where the first local minimum in the increasing branch of the magnetization curve is observed) can thus be used as qualitatively indirect information for an average value of the intergranular currents. In Fig. 10, we show this field H_J as function of temperature. It is interesting to note the linear temperature dependence of H_J from $T=T_c$ down to $T \approx 10$ mK. This temperature dependence follows neither the Ambegaokar and Baratoff result for the dc Josephson current of a superconductor-insulator-superconductor junction between classical superconductors nor the positive curvature expected for a proximity superconductor-normal-metal-superconductor junction. More work in controlled junction geometries is necessary in order to understand the Josephson effect between the unconventional superconducting phases of UPt_3 .

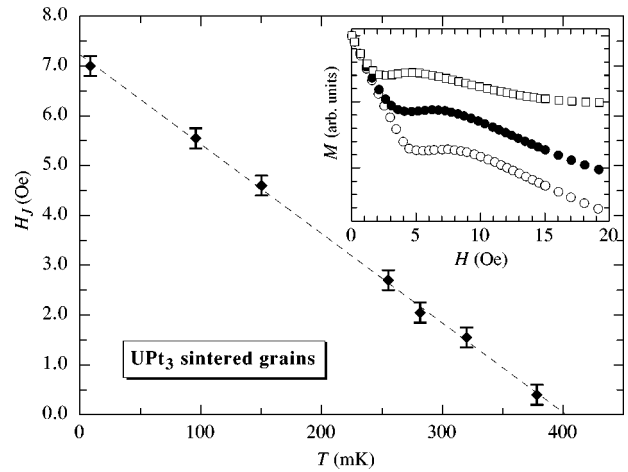


FIG. 10. Temperature dependence of the field H_J corresponding to the first local minimum observed in the increasing branch of the magnetization curve for granular UPt_3 . In the inset, the increasing branch of the magnetization cycles measured at different temperatures is shown for illustration (\circ : $T=96$ mK, \bullet : $T=150$ mK, \square : $T=255$ mK).

C. Flux dynamics

Studies of vortices and their dynamics in classical hard type-II superconductors have a long history on account of the technological importance of such materials. A type-II superconductor carrying a current is in a thermodynamically metastable state which is thus bound to decay towards equilibrium as a result of thermally activated motion of vortices. This phenomenon of vortex decay or vortex creep was observed by Kim *et al.*¹² and described by Anderson.¹³ With the discovery of the high- T_c superconductors, a new chapter in the field of vortices opened. Innumerable experimental and theoretical works appeared in the last decade describing different, fascinating phenomena not observed in classical superconductors. In particular, studies on magnetic relaxation uncovered giant creep rates on account of the high temperatures, short coherence lengths, and strong anisotropies that characterize those materials.¹⁴ Usually, the time dependence for flux creep in classical as well as in high- T_c superconductors is logarithmic or it can be described by power laws.

Here we discuss flux dynamics in a low-temperature superconductor, UPt_3 , which also shows anomalous behavior clearly different from the one observed in the classical and high-temperature superconductors. The relaxation laws in UPt_3 are significantly different. For very low fields (of the order of several Oe, i.e., of the order of the lower critical field H_{c1}), relaxation curves follow a stretched-exponential law of the form

$$M(t) - M(\infty) = [M(0) - M(\infty)] \exp[-(t/\tau)^\beta], \quad (3)$$

with a parameter β of the order of 0.6–0.7.⁵ This behavior is observed for field-on as well as for field-off measurements. In the framework of the work reported here, investigations of the relaxation of the remanent magnetization have been extended to higher fields, such that the sample is always in the fully critical state at the beginning of the decay measurement.

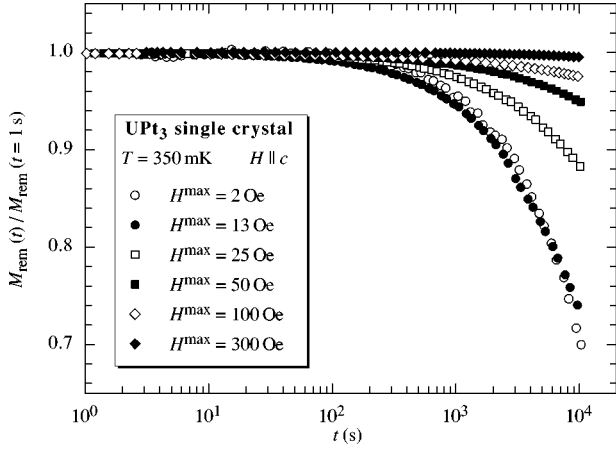


FIG. 11. Relaxation of the remanent magnetization M_{rem} of the UPt₃ single crystal with $H\parallel c$ at $T=350$ mK for different cycling fields H^{max} .

Isothermal relaxation curves of the remanent magnetization M_{rem} were taken after cycling the specimen in an external field H . In all the decay measurements of M_{rem} reported here, the specimen is first zero-field cooled to the desired temperature, then the field H is raised up to H^{max} in about 30 s and subsequently removed in about 1 s. The measurements of $M_{\text{rem}}(t)$ start typically at $t \approx 1$ s where $t=0$ has been chosen as the time when the applied field H reaches zero. The relaxation of the magnetization is typically measured in a time window $1 \text{ s} < t < 10^5$ s. After each decay measurement, the specimen is heated above its critical temperature T_c^+ and the expelled flux is recorded as function of temperature in order to obtain M_{rem} at the beginning of the decay as the sum of the decayed flux plus the flux expelled during heating.

In Figs. 11 and 12, typical relaxation measurements obtained for the UPt₃ single crystal are presented for different cycling fields H^{max} and temperatures. Figure 13 shows various relaxation curves measured at different temperatures for the sintered granular sample of UPt₃. From these curves, the following observations can be made:

(i) At a constant temperature, the relaxation is strongly dependent on the value of the cycling field H^{max} [Fig. 11]. The normalized relaxation is stronger the lower the cycling field.

(ii) At all temperatures, the fraction of the remanent magnetization which leaves the sample within a fixed time-interval is significantly bigger for the granular sample than for the single crystal [Figs. 12 and 13].

(iii) Measurements starting with the UPt₃ single crystal in the fully critical state exhibit a rather sharp increase of the short-time relaxation rate at higher temperatures ($T \geq T_c^-$), whereas for temperatures $T \leq 400$ mK no visible decay is observed at short times [Fig. 12(b)].

(iv) The short-time relaxation behavior for the granular sample of UPt₃ is clearly different and appears to be independent of temperature [Fig. 13(b)].

For the single crystal at low cycling fields, the decays can be well fitted with a stretched exponential law (3), whereas this fit does not give any meaningful results for higher cycling fields. With increasing cycling fields, the shape of the relaxation curve is more and more dominated by a contribution from a logarithmic law [$\Delta M(t) \propto \ln t$] which is visible

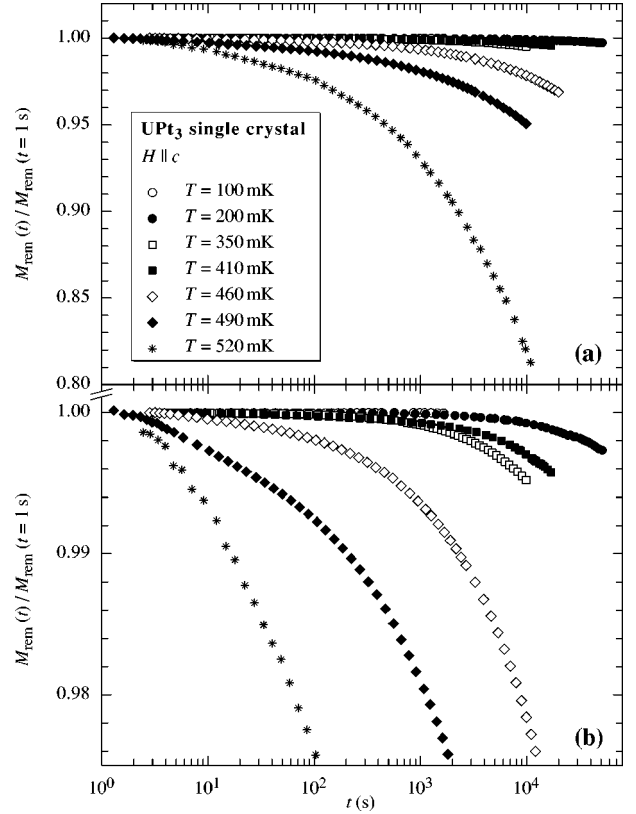


FIG. 12. Relaxation of the remanent magnetization of the UPt₃ single crystal with $H\parallel c$ at different temperatures. Note that (in addition to the strong increase of the relaxation with temperature observed at long times) a clear change in the short-time behavior can be observed for $T \geq 460$ mK. (b) Same data in an expanded vertical scale.

especially for short times ($t \lesssim 100$ s). Due to this fact, the fit to the data using expression (3) does not give satisfactory results for high cycling fields. Moreover, the fraction of the remanent magnetization which decays within a given time interval decreases with increasing cycling field.

According to the Bean model for a type-II superconductor with pinning,⁹ when a small magnetic field is applied, the flux penetrates into the sample only up to a certain distance from its surface. For high enough fields, a gradient of flux is established in the bulk of the material. Therefore, for low cycling fields one only probes the dynamics of vortices close to the surface. At larger fields, the critical state is established and the decays reflect the motion of bulk vortices as well as surface vortices. Thus, we argue that the almost pure stretched exponential law at small cycling fields results from the motion of surface vortices, while vortices in the bulk of the sample relax via a logarithmic law of the form $M(0) - M(t) \propto \ln t$. When both types of decays are present, the SQUID magnetometer which detects the total magnetic flux of the sample, measures the sum of the two. This gives a decay which, in our time window, can be described by a law of the form

$$M(t) = \Delta M^{\text{surface}} \exp[-(t/\tau)^\beta] - \Delta M^{\text{bulk}} \ln t + \text{const.} \quad (4)$$

As τ in Eq. (4) lies outside the time window for most of the measurements ($\tau > 10^5$ s), the data cannot be quantita-

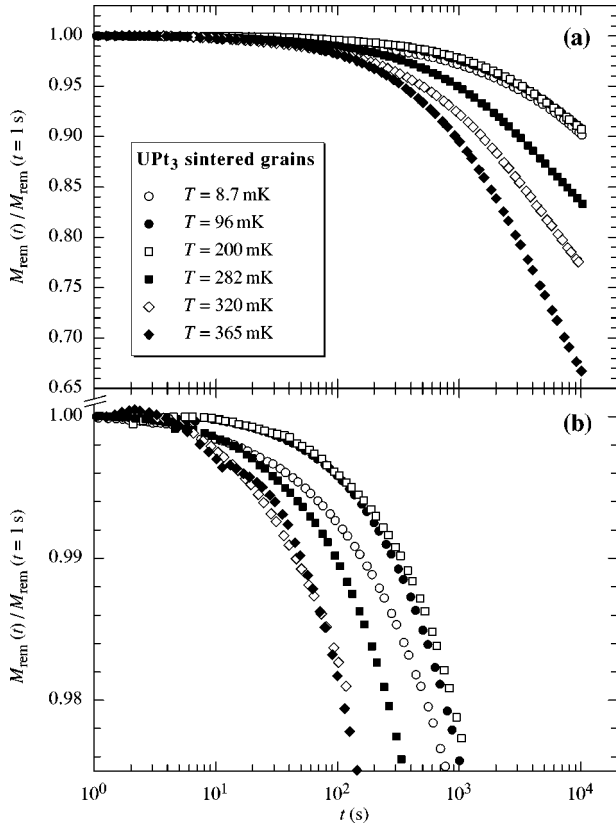


FIG. 13. Relaxation of the remanent magnetization of granular UPt_3 at different temperatures. All the measurements shown here start with the sample in the critical state. Note that the temperature dependence of the short-time relaxation behavior (lower graph with the same data in an expanded vertical scale) is significantly different from the one of the single crystal (Fig. 12).

tively fitted with expression (4) unless either the fraction $\Delta M^{\text{surface}}$ or the time τ are known. We therefore have chosen to describe the decays with two parameters, $S_{\text{initial}} = -\partial \ln M / \partial \ln t$, the initial logarithmic rate, and $\Delta M [10^4 \text{ s}]$, the deviation from a pure logarithmic decay law at $t = 10^4 \text{ s}$. As S_{initial} describes the logarithmic decay whereas the deviation ΔM is proportional to $\Delta M^{\text{surface}}$ (assuming that both, β and τ , are independent of temperature), we identify S_{initial} with the relaxation from bulk vortices and ΔM with the decay from surface vortices. In the following, decays of surface vortices and vortices in the bulk are analyzed independently using these two parameters.

Dynamics of surface vortices in UPt_3

Stretched-exponential laws describe the relaxation of a very wide range of phenomena in complex, strongly interacting materials with slow recovery towards equilibrium.¹⁵ A typical example which has been widely studied is the relaxation in amorphous or glassy materials. In UPt_3 , the question of the origin of stretched-exponential relaxation of surface vortices remains open at this moment.

The dependence of the ratio $\Delta M [10^4 \text{ s}] / M_{\text{rem}}$ on the cycling field H^{max} is illustrated in Fig. 14 using the data obtained for the single crystal at a temperature $T = 450 \text{ mK}$. The ratio $\Delta M [10^4 \text{ s}] / M_{\text{rem}}$ decreases dramatically from more than 50% for low fields to only 1% in the fully critical

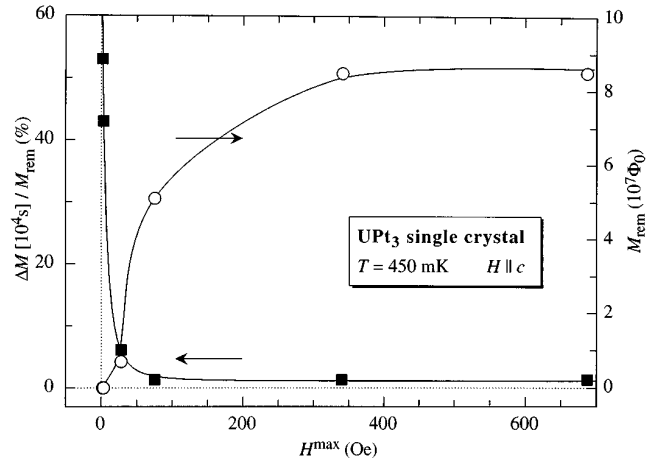


FIG. 14. Normalized fraction $\Delta M [10^4 \text{ s}] / M_{\text{rem}}$ (■, left scale) and values of the remanent magnetization M_{rem} given in number of flux quanta Φ_0 at the sample (○, right scale) for different cycling fields H^{max} . The solid lines only serve as guides to the eye.

state ($H^{\text{max}} \gtrsim 300 \text{ Oe}$ at $T = 450 \text{ mK}$).

In Fig. 15, the normalized temperature dependence of ΔM is plotted as obtained from decay measurements of the UPt_3 single crystal and the granular sample. As ΔM is normalized using the total remanent magnetization M_{rem} and not $\Delta M^{\text{surface}}$ (which is not known), the values obtained for the rate are lower estimates (see also Fig. 14). One can see clearly that, due to the much increased surface-to-bulk ratio of the granular sample as compared to the single crystal, at all temperatures the values of $\Delta M / M_{\text{rem}}$ are considerably higher for the granular sample than for the single crystal. In fact, as shown in Fig. 13, relaxation of the remanent magnetization of the granular sample showed, within our precision, practically *no* logarithmic contribution to the decay, suggesting that the width of the layer at the surface in which the vortices decay with a stretched-exponential decay law is comparable to the size of the grains. A comparison between the stretched-exponential decays in the crystal and the granu-

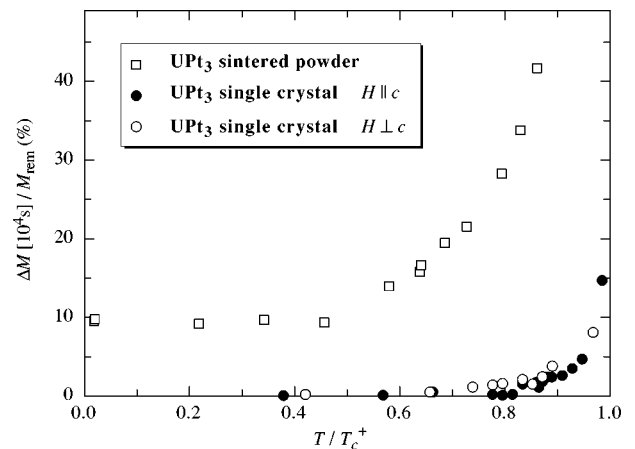


FIG. 15. Normalized fraction $\Delta M [10^4 \text{ s}] / M_{\text{rem}}$ of surface vortices in UPt_3 which have left the sample within the first 10^4 s after the start of the decay as function of the reduced temperature. All points are taken when the sample was in the fully critical state at the beginning of the measurement.

lar sample is relevant in spite of the fact that we do not have evidence for a double transition in the UPt₃ sintered powder, since this type of surface creep is observed in both the A phase as well as the B phase of the single crystal.

For both specimens, the values of $\Delta M[10^4 \text{ s}]/M_{\text{rem}}$ are independent of temperature for $T/T_c \lesssim 0.5-0.7$ with a value of 10% for the single crystal and $\approx 1\%$ for the granular sample. This indicates that this type of decay does not only result from thermal processes but also via some kind of quantum tunneling. Quantum creep of vortices has been observed at millikelvin temperatures in high- T_c superconductors¹⁶ as well as in organic superconductors.¹⁷ Typically, the normalized logarithmic creep rates $|\partial \ln M / \partial \ln t|$ at $T \rightarrow 0$ measured in those systems are of the order of 1%. These values agree well with the ones estimated from the quantum collective creep theory of Blatter *et al.*^{14,18} According to this theory, strong quantum creep rates occur in superconductors with large anisotropy $1/\varepsilon$, high normal-state resistivity ρ_n , and short coherence length ξ . A theoretical estimate of the quantum creep rate at $T \rightarrow 0$ with the corresponding values of $1/\varepsilon$, ρ_n , and ξ of UPt₃ shows that for this superconductor the logarithmic creep rates should be about 1000 times *weaker* than the rates in the high- T_c superconductors. The different relaxation law observed in UPt₃ — stretched-exponential instead of the usual logarithmic or power laws — as well as the strength of the relaxation in a given time interval cannot be explained with the existing theories of quantum creep.

It has been suggested by Sigrist, Rice, and Ueda^{3,8} that one way to probe an unconventional superconductor is to investigate surface effects. For example, in the A phase of superfluid ³He, the Cooper pair wave function adjusts in a way that the angular momentum **l** of the Cooper pair is directed perpendicularly to any wall.^{19,20} Similar effects are likely to occur in unconventional superconductors. However, the range of surface effects is rather short, order ξ_0 , so no essential effect is expected except in thin films with a thickness of a few coherence lengths.²¹ On the other hand, if a superconducting phase breaks time-reversal symmetry, such a phase can have unique properties close to domain walls and surfaces with persistent currents and vortices enclosing a nonuniversal flux quantum.⁸

In our investigation we find anomalous, fast dynamics of surface vortices in the granular sample as well as the bulk single crystal in *both* low-field superconducting phases of UPt₃. Since the high-temperature A phase is not supposed to break time-reversal symmetry, we have to conclude that other boundary phenomena are responsible for the giant creep rate of surface vortices following a stretched-exponential relaxation law.

Dynamics of bulk vortices in UPt₃

The dynamics of bulk vortices in UPt₃ also shows special features which are not observed in any other superconductor. The initial logarithmic creep rate S_{initial} of the remanent magnetization M_{rem} as a function of temperature is shown in Fig. 16. As one can see from the data, the creep rate $|\partial \ln M / \partial \ln t|$ is practically zero ($|\partial \ln M / \partial \ln t| < 10^{-5}$) up to about 400 mK for both field directions. Around this temperature it starts to increase slightly and then reaches rapidly a value of 5×10^{-3} close to T_c^+ .

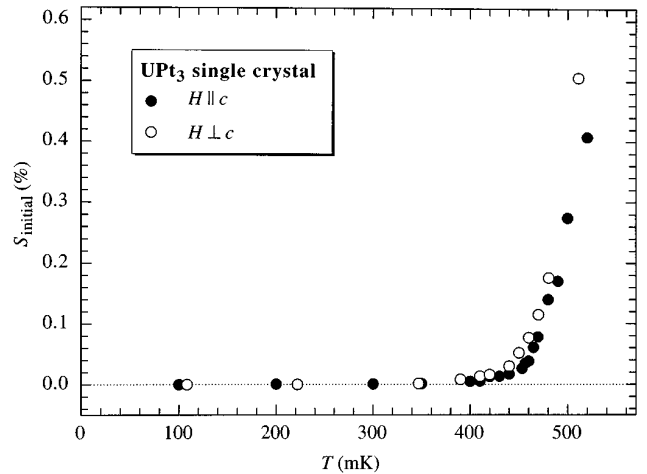


FIG. 16. Normalized logarithmic decay rate S_{initial} of bulk vortices as obtained for the UPt₃ single crystal with $H \parallel c$ (●) and $H \perp c$ (○). All points are taken with the sample in the fully critical state at the beginning of the measurement.

The very strong pinning of bulk vortices with an almost zero creep rate in the low-temperature, low-field B phase of UPt₃ cannot be the result of extrinsic quenched disorder. If this were the case, one could not explain the clear change in creep rates that occurs around 400 mK and the fast increase of the creep rates with temperature in the high-temperature A phase. The strong reduction of bulk creep in the B phase is an intrinsic property and probably related to the nature of the order parameter in this phase. In a phase that breaks time-reversal symmetry, vortices can be trapped at domain walls between domains of degenerate superconducting phases and can decay into fractional vortices carrying a noninteger multiple of the flux quantum Φ_0 . As those fractional vortices cannot exist off the domain walls, they have to recombine to give an integer flux quantum before leaving the wall. As this recombination costs energy, vortices at a domain wall will hardly ever leave the wall again, they are thus very strongly pinned by the domain wall. Due to the repulsive vortex-vortex interaction, domain walls with many trapped vortices can act as barriers for the motion of other vortices. In this way vortices can be pinned very strongly in a network of domain walls so that ordinary creep is substantially reduced.^{3,22} Note that a similar, drastic change in the pinning strength has also been observed in the lower superconducting phase of thoriated UBe₁₃.²³

Magnetic relaxation in UBe₁₃

In order to check our interpretation that the strong reduction of bulk vortex creep results from additional pinning introduced by the presence of domain walls in a time-reversal symmetry-breaking phase, similar measurements were performed on a crystal of UBe₁₃.²⁴

Some decay measurements for different cycling fields H^{max} at a constant temperature $T = 800$ mK are shown in Fig. 17. For the lowest cycling field shown in the figure, the form of the decay is similar to the ones of UPt₃. However, already for very small cycling fields, the logarithmic contribution to the decay is rather strong (of the order of several % per

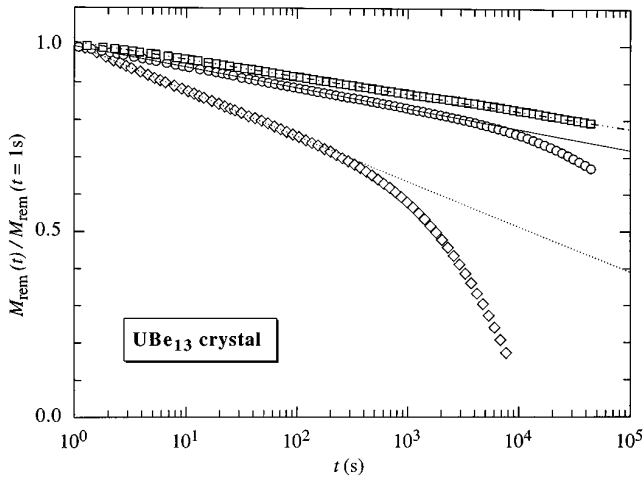


FIG. 17. Sample decay measurements of the UBe_{13} crystal taken at a temperature $T=800$ mK for three different cycling fields: $H^{\max}=3.3$ Oe (\diamond), $H^{\max}=33$ Oe (\circ), and $H^{\max}=530$ Oe (\square). The decay with $H^{\max}=530$ Oe corresponds to the case where the sample is in the fully critical state at the beginning of the decay. For each decay, a logarithmic fit through the initial data points is shown.

decade), whereas the contribution from the nonlogarithmic decay law is much smaller than for a comparable decay in UPt_3 . Moreover, the total decay is stronger in UBe_{13} than in UPt_3 . For example, for $H^{\max}=3.3$ Oe, more than 80% of the flux trapped inside the sample have left it after 10^4 s at $T=800$ mK (for UPt_3 , at a comparable reduced temperature T/T_c , this value is around 40%). For larger cycling fields — even before reaching the fully critical state when starting the decay measurement — the decay follows nearly a pure logarithmic decay law (the increase in the decay rate at longer times is still present, but this effect is so small that a quantitative analysis is not possible). Thus, it can be said that also in UBe_{13} a difference in relaxation behavior between surface and bulk vortices can be observed although the contribution of surface vortices to the total decay is much smaller than in

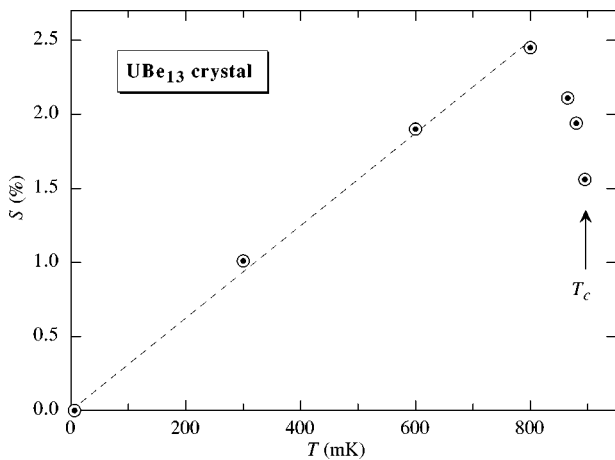


FIG. 18. Temperature dependence of $S = -\partial \ln M / \partial \ln t$, the normalized logarithmic creep rate of the UBe_{13} crystal (Ref. 24). All points have been taken after cycling the sample in a sufficiently high field H^{\max} such that the sample was in the fully critical state at the beginning of the measurement.

UPt_3 . In the following, the analysis of the decays of UBe_{13} from the fully critical state is given using a simple logarithmic decay law. In Fig. 18, the temperature dependence of the normalized logarithmic decay rate $S = -\partial \ln M / \partial \ln t$ is plotted. As can be immediately noted from the figure, the rate increases linearly with increasing temperature as is expected by the theory of thermally activated flux creep.¹³ The decrease of the rate S at high temperatures is due to the rather broad superconducting transition of the investigated sample. The temperature dependence of the logarithmic decay rate in UBe_{13} is thus significantly different from the one obtained for UPt_3 . The almost ideal pinning (creep rate $S < 10^{-5}$) of bulk vortices at lower temperatures observed in UPt_3 is therefore an effect which is not common for heavy-fermion superconductors in general, but rather an intrinsic effect of the low-temperature B phase of UPt_3 .

In preliminary relaxation measurements of the remanent magnetization in a $\text{U}_{0.9725}\text{Th}_{0.0275}\text{Be}_{13}$ single crystal, we observe a strong reduction of the normalized creep rate S below the lower transition temperature T_{c2} . The temperature dependence of S deviates clearly from the observed linear in temperature behavior for pure UBe_{13} . Since also the lower superconducting phase of thoriated UBe_{13} is believed to be characterized by an order parameter which breaks time-reversal symmetry, this result strongly supports our interpretation that the additional pinning in the B phase of UPt_3 can be attributed to effects arising due to the nature of the order parameter in that phase.

IV. SUMMARY AND CONCLUSIONS

The relaxation of the remanent magnetization in UPt_3 shows different behavior for vortices close to the surface of the specimen and vortices in the bulk. Surface vortices decay via a stretched-exponential decay law. Their decay rate is temperature independent for $T \lesssim 0.5 T_c^+$ with a rather high rate (10% of the trapped flux decaying within the first 10^4 s in the sintered sample), indicating that some new form of quantum tunneling is involved.

Moreover, the relaxation of bulk vortices shows new features which, up to now, have not been observed for any other superconductor: for the UPt_3 single crystal, the normalized creep rate $S = -\partial \ln M / \partial \ln t$ is practically zero ($S < 10^{-5}$) for temperatures up to about 400 mK. On further raising the temperature it starts to increase rapidly reaching a value of about 5×10^{-3} close to T_c^+ . As the reduction in bulk creep occurs approximately below the lower transition temperature T_c^- (the existence of which has been verified by measuring the specific heat of the sample), it is obvious to relate this additional pinning to some novel effect in the low-field low-temperature superconducting B phase of UPt_3 . This behavior can be attributed to the nature of the order parameter in the B phase of UPt_3 . In a phase that breaks time-reversal symmetry, fractional vortices get trapped and strongly pinned on domain walls between domains of degenerate superconducting phases. Due to the repulsive vortex-vortex interaction, these vortices also inhibit the motion of ordinary vortices resulting in additional strong pinning.^{3,22} Thus, the ideal bulk pinning in the B phase of UPt_3 supports scenarios that have

proposed for this phase a superconducting order parameter that breaks time-reversal symmetry.

Further support for the above conclusion was inferred from very sensitive measurements of the ac magnetic susceptibility χ . Well below and clearly separated from the superconducting transition at T_c^+ , a small peak in χ'' was detected. While the width and the position of the peak's maximum are very sensitive to the amplitude of the applied ac measuring field H_{ac} , its upper onset is nearly independent of H_{ac} . In agreement with the measured lower transition temperature T_c^- as determined from specific-heat measurements, we identify the onset of dissipation with the lower superconducting transition from the A to the B phase. We interpret the peak as resulting from losses due to the motion of domain walls and/or fractional vortices building up in the B phase. On just entering this phase from higher temperatures, the walls and

vortices may adjust to the externally applied field whereas deep inside the B phase they become strongly pinned and thus behave rigidly.

ACKNOWLEDGMENTS

For providing the $U\text{Pt}_3$ samples, we wish to thank Y. Dalichaouch, P.E. Armstrong, Z. Fisk, and R. Chau; the $U\text{Be}_{13}$ crystal has been kindly provided by M.V. Mitin. We are grateful to P. Visani, R. Vollmer, S. Wanka, and T. Pietrus for their contribution to some of the experiments reported in this work. Very valuable and fruitful discussions with M. Sigrist, T.M. Rice, R. Joynt, and D. Rainer are acknowledged. Part of this work was supported by the Swiss National Science Foundation and the U.S. National Science Foundation under Grant No. DMR-94-08835.

*Present address: UCSD, IPAPS-0360, 9500 Gilman Drive, La Jolla, CA 92093-0360.

¹H. v. Löhneysen, *Physica B* **197**, 551 (1994), and references therein.

²G. M. Luke, A. Keren, L. P. Le, W. D. Wu, Y. J. Uemura, D. A. Bonn, L. Taillefer, and J. D. Garrett, *Phys. Rev. Lett.* **71**, 1466 (1993).

³M. Sigrist and K. Ueda, *Rev. Mod. Phys.* **63**, 239 (1992), and references therein.

⁴A double-peak structure in χ'' was observed by P. Signore *et al.* [*Phys. Rev. B* **45**, 10 151 (1992)]. However, their result exhibits important differences from the data reported here: their second peak in χ'' at $T \approx 470$ mK has about the same size as the peak at higher temperature (at $T \approx 525$ mK). Moreover, the width of the transition as measured by χ' suggests that their second peak is more likely the result of a shoulder in their rather broad transition into the superconducting state (starting at $T \approx 530$ mK and being nearly finished at $T \approx 440$ mK) than a sign of the lower transition at T_c^- as proposed by the authors. In the data reported here, the diamagnetic shielding is already total at $T \approx 500$ mK, ruling out the possibility that the second peak in χ'' below $T \approx 480$ mK results from a wide superconducting transition.

⁵A. Pollini, A. C. Mota, P. Visani, G. Juri, and J. J. M. Franse, *Physica B* **165&166**, 365 (1990).

⁶R. B. Goldfarb, A. F. Clark, A. I. Braginski, and A. J. Panson, *Cryogenics* **27**, 475 (1987).

⁷K.-H. Müller, *Physica C* **159**, 717 (1989).

⁸M. Sigrist, T. M. Rice, and K. Ueda, *Phys. Rev. Lett.* **63**, 1727 (1989), and references therein.

⁹C. P. Bean, *Phys. Rev. Lett.* **8**, 250 (1962); *Rev. Mod. Phys.* **36**, 31 (1964).

¹⁰B. S. Shivaram, J. J. Gannon, Jr., and D. G. Hinks, *Phys. Rev. Lett.* **63**, 1723 (1989).

¹¹Z. Zhao, F. Behroozi, J. B. Ketterson, Y. Guan, B. K. Sarma, and D. G. Hinks, *Physica B* **165&166**, 345 (1990).

¹²Y. B. Kim, C. F. Hempstead, and A. R. Strnad, *Phys. Rev. Lett.* **9**, 306 (1962).

¹³P. W. Anderson, *Phys. Rev. Lett.* **9**, 309 (1962); P. W. Anderson and Y. B. Kim, *Rev. Mod. Phys.* **36**, 39 (1964).

¹⁴G. Blatter, M. V. Feigel'man, V. B. Geshkenbein, A. I. Larkin, and V. M. Vinokur, *Rev. Mod. Phys.* **66**, 1125 (1994), and references therein.

¹⁵H. Scher, M. F. Schlesinger, and J. T. Bandler, *Phys. Today* **44** (1), 26 (1991).

¹⁶A. C. Mota, A. Pollini, P. Visani, K. A. Müller, and J. G. Bednorz, *Phys. Rev. B* **36**, 4011 (1987).

¹⁷A. C. Mota, G. Juri, P. Visani, T. Teruzzi, K. Aupke, and B. Hilti, *Physica C* **185-189**, 343 (1991).

¹⁸G. Blatter, V. B. Geshkenbein, and V. M. Vinokur, *Phys. Rev. Lett.* **66**, 3297 (1991).

¹⁹V. Ambegaokar, P. G. de Gennes, and D. Rainer, *Phys. Rev. A* **9**, 2676 (1974).

²⁰A. J. Leggett, *Rev. Mod. Phys.* **47**, 331 (1975).

²¹N. Ogawa, M. Sigrist, and K. Ueda, *Physica B* **206&207**, 634 (1995).

²²Manfred Sigrist (private communication).

²³R. J. Zieve, T. F. Rosenbaum, J. S. Kim, G. R. Stewart, and M. Sigrist, *Phys. Rev. B* **51**, 12 041 (1995).

²⁴A. Amann, P. Visani, K. Aupke, A. C. Mota, M. B. Maple, Y. Dalichaouch, P. E. Armstrong, Z. Fisk, and A. V. Mitin, *Physica C* **235-240**, 2443 (1994).